ACS APPLIED MATERIALS & INTERFACES

Research Article

www.acsami.org

Strong and Optically Transparent Films Prepared Using Cellulosic Solid Residue Recovered from Cellulose Nanocrystals Production Waste Stream

Qianqian Wang,[†,‡] J. Y. Zhu,*[,‡] and John M. Considine[‡]

[†]State Key Lab of Pulp and Paper Engineering, South China University of Technology, Guangzhou, China

[‡]USDA Forest Service, Forest Products Laboratory, Madison, Wisconsin 53726, United States

ABSTRACT: We used a new cellulosic material, cellulosic solid residue (CSR), to produce cellulose nanofibrils (CNF) for potential high value applications. Cellulose nanofibrils (CNF) were produced from CSR recovered from the hydrolysates (waste stream) of acid hydrolysis of a bleached Eucalyptus kraft pulp (BEP) to produce nanocrystals (CNC). Acid hydrolysis greatly facilitated homogenization to fibrillate CSR to CNF with only 15 passes in a microfluidizer compared with at least 47 passes to fibrillate BEP to nanofibrils. CNF from CSR were nanowhiskers with a length between 50 and 400 nm and a diameter 3−10 nm with limited aggregation while CNF from BEP were entangled networks of nanofibrils with a length of 500−1000 nm and a diameter of 10−50 nm. CNFs from CSR had good spectral transparency from UV to infrared, i.e, transmittance of CNF-CSR suspensions at 0.1% solids consistency is greater than 90% at wavelengths greater than 340 nm, compared with less than 30% for CNF suspension produced from BEP. Specific tensile strength and modulus of CNF films from CSRs reached 75 kN·m/kg and 12 MN·m/kg, respectively, approximately 175% of the respective values for conventional paper made of refined BEP.

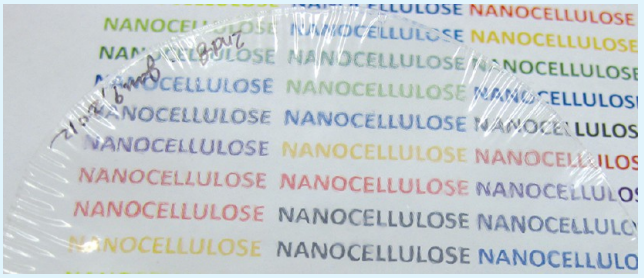

KEYWORDS: *cellulose nanocrystals (CNC), cellulose nanofibrils (CNF), transparent nanocellulose film, tensile strength, acid hydrolysis, nanowhiskers*

INTRODUCTION

Cellulose nanocrystals (CNCs), rod-like crystalline particles isolated from cellulose, have attracted great attention in the materials research community[1−3] because CNCs have unusual mechanical properties for natural materials, e.g., a theoretical tensile modulus of approximately 140 GPa[4] and a specific tensile strength of 5000 kN·m/kg,[5] or approximately 17 times that of titanium. CNCs also have very unique optical and self-assembly properties.[1,6−8] These properties offer significant potential for developing functionalized optical products and lightweight nanocomposites for a variety of applications. Furthermore, cellulose is abundant in nature, is renewable, and can be sustainably produced. However, few methods have been developed to isolate CNCs from cellulose. The strong acid hydrolysis process developed in the 1950s[9,10] has remained the most viable process for producing CNCs. Using sulfuric acid at concentration around 60 wt % produces CNCs in stable colloidal suspension due to sulfate groups formed that impart electrostatic stability to CNCs which facilitate aqueous processing.[10,11] Unfortunately, strong acid hydrolyzes a significant amount of cellulose into sugars which results in low CNC yield between 30 and 50%.[12,13] Moreover, sulfation of cellulosic solids, reduction in degree of polymerization (DP), and production of CNCs during strong acid hydrolysis occur abruptly and simultaneously when acid hydrolysis parameters are varied, which makes significant cellulose loss to sugars unavoidable.[12−14] Recovery of soluble sugar in the strong acid stream is not economically possible. Loss of cellulose during acid hydrolysis due to saccharification represents a significant problem to the CNC production process.

We have successfully identified a narrow operating window to avoid cellulose saccharification to achieve near zero cellulose loss to soluble sugars in CNC production using sulfuric acid.[14] In this narrow operating window we were able to simultaneously recover CNC and cellulosic solid residue (CSR) which had not been reported in the literature.[12,13] Equivalent CNC yield of as high as approximately 55% to that obtained under conventionally considered optimal conditions was achieved; in addition, a CSR yield of 15% or higher was achieved using a bleached Eucalyptus kraft pulp (BEP). CNCs produced in this operating window were found to be no different from those produced using the conventional "optimal" conditions. Furthermore, CSR had a good degree of sulfation that facilitated further mechanical fibrillation to produce cellulose nanofibrils (CNF) suitable for aqueous processing. As expected, CNFs from CSR had longer aspect ratios than

Received: December 11, 2012
Accepted: March 8, 2013
Published: March 8, 2013

   dx.doi.org/10.1021/am302967m | *ACS Appl. Mater. Interfaces* 2013, 5, 2527−2534

CNCs. Therefore, CSR and CNFs derived from CSR represent a new cellulosic material that has potential for a variety of applications.

Many studies have reported CNF production from lignocelluloses using different mechanical fibrillation processes,[15] such as homogenization,[16−18] microfluidization,[19,20] and disk grinding.[21,22] The production process affects properties of the resultant CNFs; microfluidization and grinding produces better mechanical properties than homogenization.[15] Pretreatment of wood fibers prior to mechanical fibrillation has significant impact on the CNF properties. TEMPO-mediated oxidation of fibers significantly reduces energy input for subsequent mechanical fibrillation and produces relatively uniform CNFs with excellent optical transparency.[23] Enzyme pretreatments can also reduce energy consumption in mechanical fibrillation and produce less aggregated CNFs but with lower mechanical strength than those without enzyme pretreatments.[19,24]

The objective of this study is to evaluate the physical, mechanical, and optical properties of CNFs derived from CSR. Specifically, neat films made of CNFs from CSRs recovered from CNC hydrolysates (waste stream) under two strong acid hydrolysis conditions were compared with neat films made of CNF produced from direct mechanical fibrillation of the same BEP. The results indicate that the CNFs from CSR had interesting properties that suggest significant potential for high value utilization. The goal of this study is to technically justify the practice of CNC production process conditions that we have identified[14] and the recovery of CSR from the waste stream of this new CNC production process. This practice conserves raw materials and reduces CNC production cost. This work also implies that acid hydrolysis may be applied as a stand-alone pretreatment to significantly reduce energy consumption in mechanical fibrillation to produce CNFs.

MATERIALS AND METHODS

Raw Materials. Sulfuric acid of ACS reagent grade was purchased from Sigma-Aldrich (St. Louis, MO). Bleached eucalyptus kraft dry lap pulp (BEP) was obtained from Aracruz Cellulose (Brazil). BEP is commercially available in large quantities throughout the world and was used in our previous studies[14,21] on CNC and CNF production. Chemical analysis of the BEP showed Klason lignin 0.1 ± 0.1%, glucan 78.1 ± 1.0%, and xylan 15.5 ± 0.6%. BEP was first soaked in deionized (DI) water for 12 h and then disintegrated with a laboratory disintegrator (TMI, Ronkonkoma, NY) using 10 000 revolutions. Resultant BEP fibers had a weighted length and width of approximately 0.8 mm and 25 μm, respectively (Figure 1a). Disintegrated BEP was kept in a cold room at 4°C until use. Two CSR samples were recovered from the waste streams (hydrolysates) of two respective experiments of CNC production by acid hydrolysis using the disintegrated BEP as described in the following section.

Recovery of CSR from the Waste Stream of CNC Production. Strong acid hydrolysis of BEP were conducted at two sets of conditions listed in Table 1: (60, 40, 70) and (58, 56, 40) for the production of CNC as described previously[14] where hydrolysis conditions are expressed in the form of (sulfuric acid in wt %, temperature in °C, and hydrolysis duration in min). Oven dry weight (OD) of 30 g of BEP was used for each acid hydrolysis experiment. A water bath was used to control the temperature of acid hydrolysis to approximately ±2 °C. Mechanical shear mixing was applied at 200 rpm during hydrolysis. At the end of designated hydrolysis time, 10-fold of DI water was used to quench hydrolysis. The suspension was vigorously stirred for 10 min and then washed and repeatedly centrifuged at 9 000 rpm or approximately 13 200*g* (Sorvall Superspeed RC2-B, 5.75 inches rotator, Ivan Sorvall, Inc., Norwalk, CT) to remove excessive sulfuric acid until turbid. After dialysis for a week, the

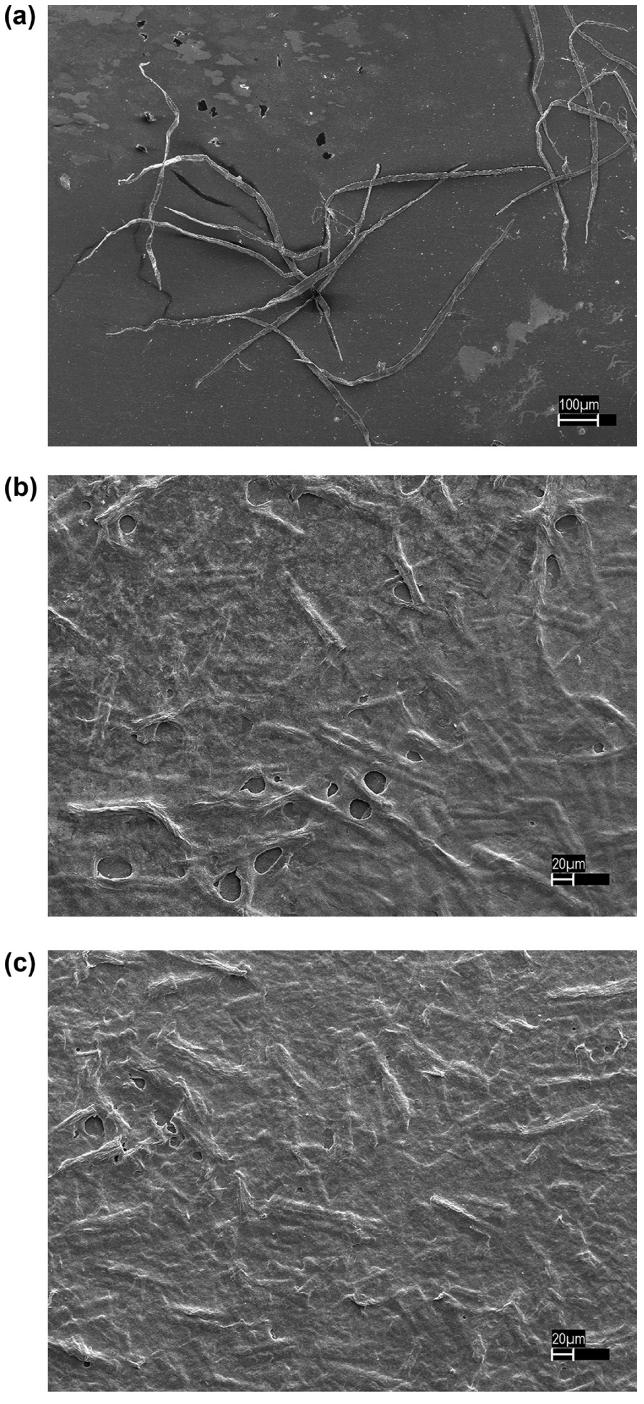

Figure 1. SEM images of the original BEP fibers and cellulosic solid residue (CSR) from two acid hydrolysis conditions (Table 1): (a) BEP, (b) CSR-I, and (c) CSR-II.

Table 1. Hydrolysis Conditions and Yields of CNC and CSR from Two Acid Hydrolysis Experiments

	CSR I	CSR II
sulfuric acid (wt %)	60	58
temperature (°C)	40	56
duration (min)	70	40
CNC yield (%)	33.0	29.9
CSR yield (%)	44.1	55.4

suspension underwent a treatment in an ultrasonic bath (model FS21H, Fisher Scientific) with ice for 15 min to disperse the cellulose nanocrystals. The CSR from acid hydrolysis was separated from CNC (supernatant) by centrifugation for 10 min at 13 200*g* at a solids consistency less than 0.3 wt %.

Volumes and weights of separated CNC and CSR were recorded for yield determinations. Consistencies of the two cellulose suspensions after CNC and CSR separation were determined as described in our previous study[14] using a COD (chemical oxygen demand) method.[25] Aliquots of CNC or CSR samples were digested in COD test vials (Biosciences, Inc., Bethlehem, PA). The amount of chromium consumed as measured from absorption at 600 nm by a UV−vis spectrophotometer (Spectronic Genesys 5, Milton Roy Company, Warminster, PA) was used to determine COD. Cellulose concentration in the suspension can be calculated from the measured COD through calibration using Avicel:

$$C_{C_6H_{10}O_5}(\mathrm{mg/L}) = \mathrm{COD}/1.185 = 2877.6I^{600} \quad (1)$$

Production of Cellulose Nanofibrils (CNF). Recovered CSRs were used to produce CNFs, designated CNF-CSR I and CNF-CSR II (Table 2). Three types of CNF from the original BEP were also produced so that comparisons of mechanical and optical properties can be made among different CNFs. Production of CNFs was conducted according to the schematic flow diagram shown in Figure 2.

Table 2. Description and Degree of Polymerization (DP) and Crystallinitiy Index (CrI) of Different Cellulose Nanofibrils (CNFs)

identification	CNF production method	DP	CrI
BEP		843	61.1 ± 0.6
CNF-CSR I	15 passes microfluidization	282	41.3 ± 0.5
CNF-CSR II	15 passes microfluidization	298	46.0 ± 0.5
CNF-M-47p	47 passes microfluidization	354	40.3 ± 0.1
CNF-S7h	7 h SuperMassColloider milling	611	43.4 ± 0.2
CNF-S11h	11 h SuperMassColloider milling	475	40.4 ± 0.2

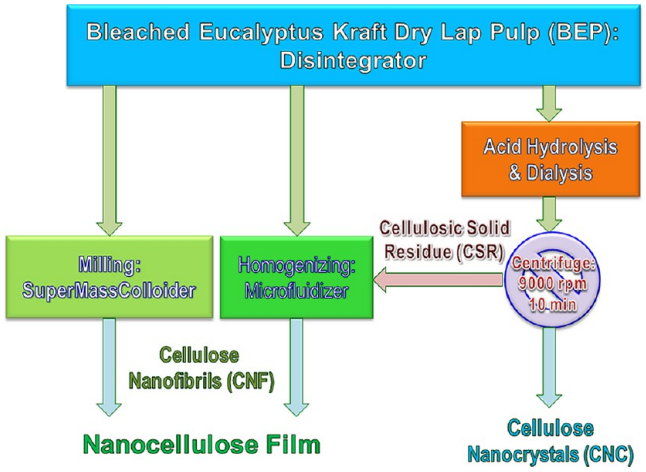

Figure 2. Experimental schematic flow diagram illustrating different production processes of cellulose nanofibrils (CNFs).

Both a microfluidizer (model M-110EH-30, Microfluidics, Newton, MA) and a SuperMassColloider (model MKCA6-2, disk model MKGA6-80#, Masuko Sangyo Co., Ltd., Japan), a stone disk mill/grinder, were used for the production of CNFs using different feedstocks. CNFs from CSR were produced only using the microfluidizer because of the small amount of materials available. Therefore, CNFs were produced from both the microfluidizer and the SuperMassColloider using the original BEP for comparison.

CSR samples, CSR I and CSR II (Table 1), were fed into the microfluidizer at 2 wt % solids. The CSR suspension was processed for 10 passes through a 200 μm chamber and subsequently for 5 passes through an 87 μm chamber and became gelation, suggesting the CSR has been refined to nanofibrils.

CNF-M47P was produced by homogenizing the original BEP in the microfluidizer at 0.3 wt % fiber consistency. Its long fibers (Figure 1a) prevented it from being processed at higher consistency. A total of 47 passes in the 200 μm chamber were required to delaminate the fibers into nanofibrils. CNF-S7h and CNF-S11h were produced from the original BEP in the SuperMassColloider according to the procedure described previously.[21] A mass of 200 g of OD BEP was used to make a pulp suspension at consistency 2.0 wt %. The suspension was directly fed into the SuperMassColloider. The initial stone disk plate gap was set at −100 μm; pulp suspension prevented contact between the two stones in milling even at the negative initial plate gap setting. The suspension was circulated through the SuperMassColloider using a peristaltic pump for continuous processing. Milling was terminated at two designated time to produce CNFs with different levels of fibrillation, i.e., 7 h (CNF-S7h) and 11 h (CNF-S11h). The original BEP was also beaten by a valley beater (Valley Laboratory Equipment, Voith, Appleton, WI) to 300 mL of Canadian Standard Freeness (CSF). Conventional handsheets were prepared using the TAPPI Standard Method T205 sp-06.[26]

Degree of Polymerization (DP) and Crystallinity Index. CNF DPs were determined according to the TAPPI Standard Test Method T230 om-08.[26] Viscosities of the CNF solutions were measured by a capillary viscometer, and DP was calculated according to eq 2[27,28]

$$\mathrm{DP}^{0.905} = 0.75[954\log(x) - 325] \quad (2)$$

where x is the viscosity of the CNF solution.

The crystallinity indices (CrI) were calculated by eq 3 following an FT-Raman spectroscopic method[29] based on the ratio of measured Raman spectral intensities at 380 cm^{-1} and 1096 cm^{-1}

$$\mathrm{CrI}^{\mathrm{Raman}} = \left[\frac{I_{380}}{I_{1096}} - 0.0286\right]/0.0065 \quad (3)$$

Electron Microscopy. Scanning electron microscopy (SEM) images were taken by drying a small amount of suspension on a polished aluminum mount and sputter-coating with gold to provide adequate conductivity. Samples were imaged and photographed using a Leo EVO 40 SEM. Transmission electron microscopy (TEM) images of CNF from CSR were measured by the Purdue Technology Center at Purdue University (West Lafayette, IN). TEM images of the CNF from the original BEP were measured at SAIC-Frederick, Inc., National Cancer Institute (Frederick, MD). Samples were diluted to solids consistency of approximately 0.1% and then analyzed. Each aqueous sample was adsorbed to freshly glow-discharged support grids (with carbon-coated formvar film) for 30 s, then rinsed with water and negatively stained with 0.5% uranyl acetate. Images were recorded on a Hitachi H7650 microscope at 80 kV with a 2k × 2k AMT CCD camera at SAIC-Frederick and on a Philips CM-100 microscope utilizing 100 kV accelerating voltage and a 2k SIA CCD camera at the Purdue Technology Center.

Measurements of Optical Properties. A UV−vis spectrophotometer (model 8453, Agilent Technologies, Palo Alto, CA) was used to measure the spectral transparency of different CNF suspensions using transmittance mode. A thoroughly mixed aliquot of CNF suspension was diluted to 0.1 wt % and placed in a 10 mm quartz cuvette. Optical opacity of the CNF films were measured by the standard TAPPI Test method TAPPI T 519 om-06.[26]

Preparation and Testing of CNF Films. CNF suspensions were diluted to 0.1 wt % and stirred for 12 h. Neat films were formed by ultrafiltration of diluted CNF suspensions using a Millipore hazardous waste filtration system assisted with compressed air for 12 h. The filtration membrane was 0.22 μm Durapore membrane (Millipore, GVWP14250, Ireland) with a 142 mm diameter and open area of 100 mm. Wet films were pressed with a membrane and blotter paper for 3 min at 207 kPa (30 psi) and for another 3 min at 345 kPa (50 psi).

Films were dried for 24 h at 60 °C under 14 kPa pressure. Prior to mechanical testing, films were pre-conditioned for 24 h at 30% relative humidity and 27 °C, followed by conditioning at 50% relative humidity and 23°C for another 24 h. Tensile tests were conducted using an Instron system (model 5865, Norwood, MA) equipped with a laser extensometer for precise displacement determination (Laser Extensometer LX500, MTS System Corporation, Eden Prairie, Minnesota). Rectangular tensile specimens were 15 mm wide and had an extensometer gauge length of 37 mm and nominal grip length of 60 mm.

RESULTS AND DISCUSSION

CSR Morphology. SEM images show CSR fibrils from two sets of acid hydrolysis conditions have a nominal length of 100 μm and width of 20 μm (Figure 1b,c), much shorter than the 0.8 mm length-weighted length of the original BEP fibers (Figure 1a). Acid hydrolysis tends to cut the cellulose chain length. Length of the BEP fibers were confirmed by a commercial fiber quality analyzer (FQA-360, OpTest Equipment Inc., Hawkesbury, ON, Canada). However, the length of CSR fibers were below the sensitivity of the fiber quality analyzer.

Optical, Morphological, and Structural Properties of CNF Derived from CSR. CNF suspensions prepared from CSR and those prepared from the original BEP were visibly different (Figure 3). CNFs from CSR appeared optically

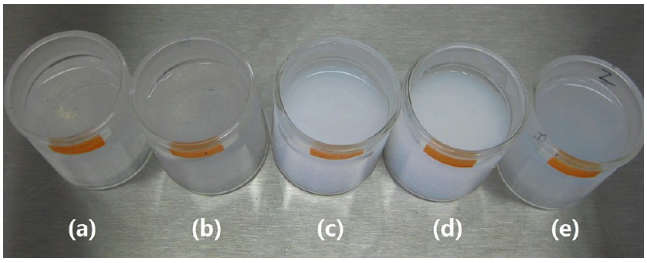

Figure 3. Visual images of different cellulose nanofibril (CNF) suspensions at a solid consistency of 1.5% except for suspension e at 0.3%: (a) CNF-CSR I, (b) CNF-CSR II, (c) CNF-S7h, (d) CNF-S11h, and (e) CNF-M-47p at 0.3%.

transparent while CNFs from the original BEP using the SuperMassColloider were milky white with a slight bluish color, and CNFs from the original BEP fibrillated by the microfluidizer had a light blue color (notice the difference in consistency, see the caption for Figure 3). Spectral transmittance measurements (Figure 4) agreed with visual observations. Spectral transmittance at 0.1% solids consistency of CNF-CSR I and CNF-CSR II were greater than 90% from wavelength 340 nm to 1100 nm (visible to infrared). Transmittance was above 99% in the infrared region (>700 nm). Even in the UV range (>220 nm), spectral transmittance was greater than 50%. In comparison, spectral transmittance of the CNF suspensions at the same consistency produced from the original BEP, CNF-M47p, CNF-S-7h, and CNF-S11h, were lower (Figure 4). Maximal transmittance at 1100 nm was at 80% for CNF-M-47p and less than 40% for CNF-S-7h and CNF-S11h. Homogenization at low consistency of 0.3% solids in the microfluidizer was much more effective to increase light transmittance than milling at 2% solids consistency. Extended milling of BEP from 7 h to 11 h did not significantly improve spectral transmittance (Figure 4). This suggests that the particular stone used in the SuperMassColloider may have

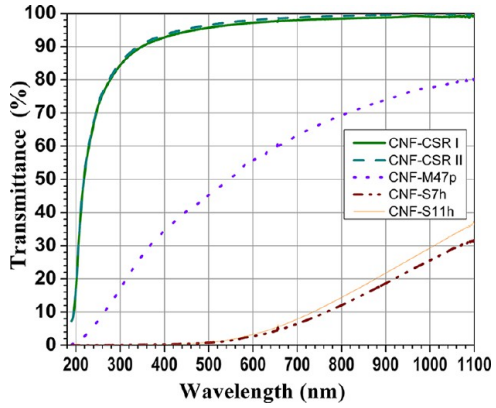

Figure 4. Spectral transmittance of different cellulose nanofibril (CNF) suspensions at 0.1% consistency.

reached its limit to further delaminate fibrils as confirmed by TEM images and corroborated by a previous study.[21] Close to zero transmittance below wavelength 500 nm gave a bluish color for these two CNFs. Transmittance of CNF-M47p below wavelength 500 nm is less than 45%. The more bluish color of CNF-M47p than CNF-G7h and CNF-G11h was due to its relatively higher transmittance (lower absorption) in the yellow to infrared range (Figure 4).

TEM was used to evaluate the morphologies of the CNFs produced from CSR. Visual observation indicated morphological differences among the three types of CNFs (Figure 5). CNFs produced from CSRs were individually separated whiskers with relatively uniform diameters in the range of 3–10 nm. Length and aggregation of the whiskers however depends on CSR, i.e., lengths of CNF-CSR-I were approximately 50–250 nm (Figure 5a) and were shorter than lengths of CNF-CSR II, approximately 200–400 nm (Figure 5b). CNF-CSR I had almost no aggregation, probably caused by the degree of acid hydrolysis of the initial BEP in CNC production. A lower yield of CSR-I as compared to CSR-II (Table 1) suggests that the acid hydrolysis in CSR-I was more astringent than in CSR-II. However, longer CNF-CSR-II whiskers did not reduce its optical properties (Figure 4), suggesting the length and degree of aggregation of CNF-CSR II is still close to or within the range of spectral wavelength (200–1100 nm) tested. In contrast, morphologies of the CNFs from the original BEP were entangled fibril networks (Figure 5c–e). Fibrils were in the form of fibril bundles of different diameters with incomplete separation. The fibril network size, especially for CNF-S7h and CNF-S11h, was larger than the spectral wavelength tested in Figure 4. It appears that entanglement was more severe for CNF-S7h (Figure 5d) and CNF-S11h (Figure 5e) than that of CNF-M47p (Figure 5c). Examination of the fibril length helped explain observed differences in the spectral transmittance in Figure 4.

We can estimate the degree of entanglement of the CNF suspension using the crowding factor shown in eq 1[30−32] based on TEM measured fibril length and diameter.

$$N = \frac{2}{3} C_V \left(\frac{L}{d}\right)^2 \tag{4}$$

where N is the crowding factor in the CNF suspension or the number of fibrils in the volume of a sphere with diameter equal to the length of the fibril, C_V is the volumetric concentration of fibrils, L and d are the (average) length and diameter of the

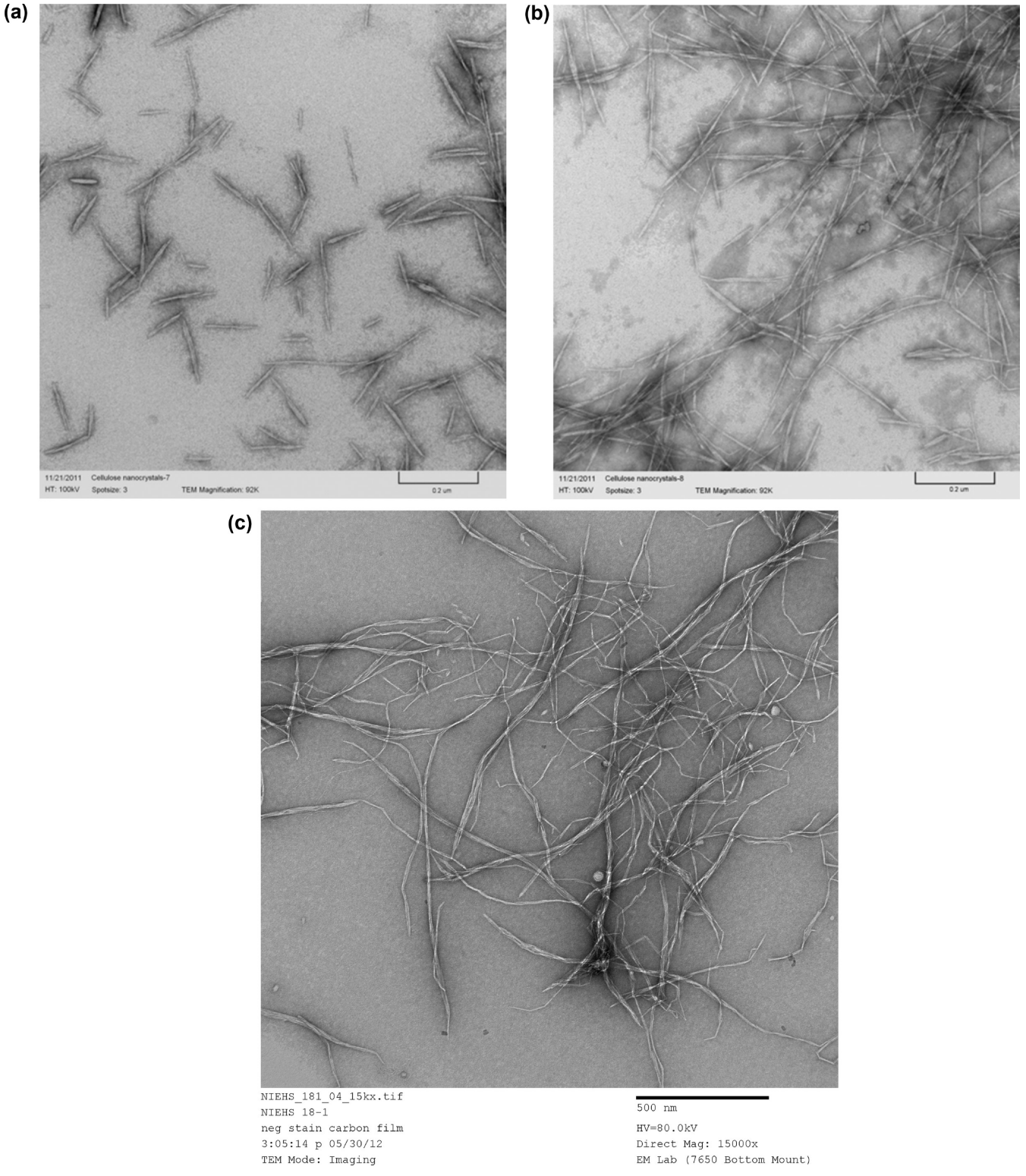

Figure 5. continued

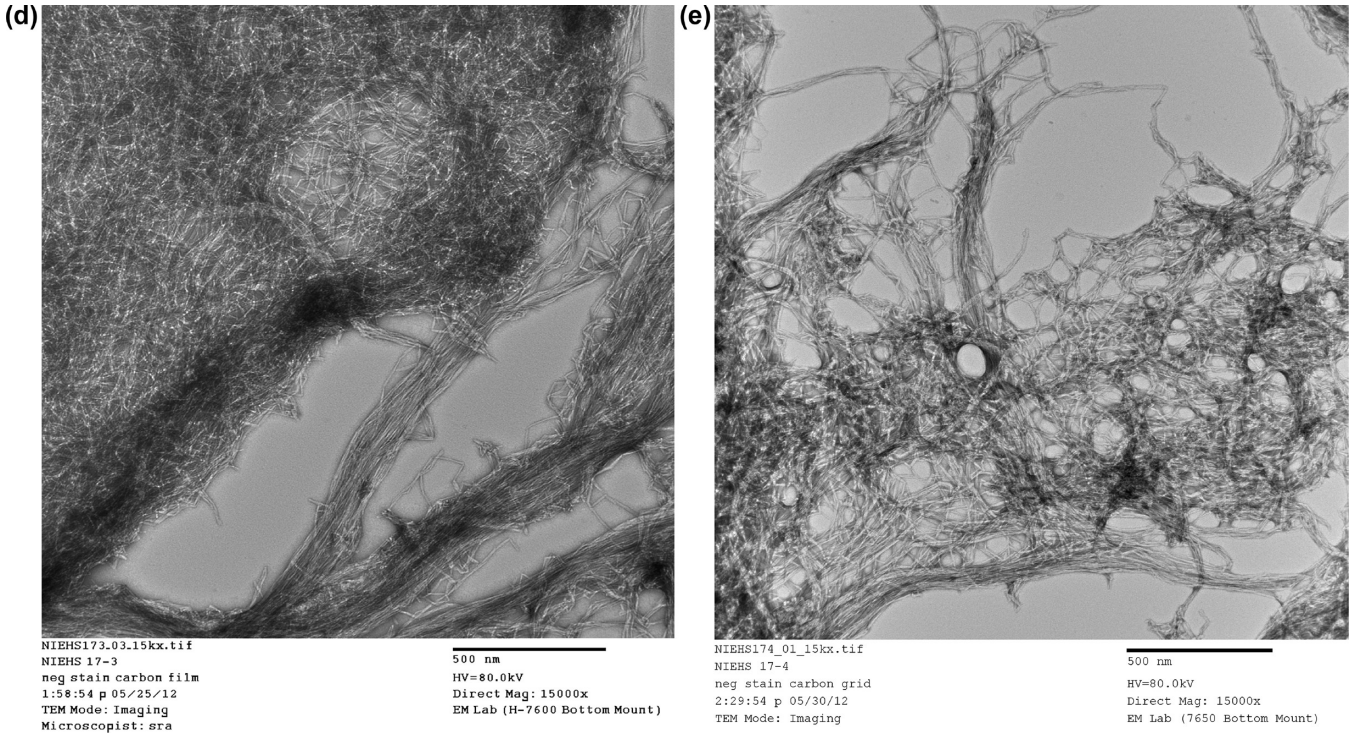

Figure 5. TEM images of different cellulose nanofibrils (CNFs): (a) CNF-CSR I, (b) CNF-CSR II, (c) CNF-M-47p, (d) CNF-S7h, and (e) CNF-S11h. Scale bars = 200 nm for parts a and b; scale bars = 500 nm for parts c–e.

CNF, respectively. We can assume that fibrils do not have lumens and so have a density equal to that of the cellulose fiber cell wall of approximately 1.5 kg/m^3. The crowding factor for CNF can be expressed as

$$N_{\text{fibrils}} = C_{\text{m}}\left(\frac{L}{d}\right)^2 = C_{\text{m}}x^2 \tag{5}$$

where C_{m} is the mass concentration in the fibril suspension or solids consistency and x is the average fibril aspect ratio. Celzard et al. established that a crowding factor of 16 is the criterion for fiber connectivity or "gel crowding factor".[32] Therefore, we can determine the critical mass concentration (solid consistency) for CNF gelation as

$$C_{\text{m}} = 16\left(\frac{d}{L}\right)^2 = \frac{16}{x^2} \tag{6}$$

Average aspect ratios were about 30 and 60 for CNF-CSR-I and CNF-CSR-II, respectively. Therefore, the critical solids consistency to form a gel can be estimated as 1.8% and 0.4%, respectively, for these two CNFs. This estimate cannot be applied to CNFs that are not individual fibrils, such as those shown in in Figure 5c–e.

DP and CrI of the CNFs were measured to evaluate the physico-chemical structural properties of the CNFs shown in Figure 3. DP and CrI of all CNFs were significantly decreased by mechanical fibrillation (Table 2). DP of CNF-CSR I and CNF-CSR II were approximately the same, suggesting the difference in acid hydrolysis conditions were overcome by homogenization after 15 passes. Acid hydrolysis facilitated further DP reduction which resulted in low DP of approximately 300 for CNFs from CSRs. Homogenization at 0.3% consistency resulted in more drastic reduction in DP than milling at 2% in the SupermassColloider as seen from the difference in DP between CNF-M47p and CNF-S7h or CNF-S11h. Longer milling time produced a lower DP. Typical DP of CNC is approximately 120 or less.[13]

CrI of all CNF samples were significantly reduced from the original BEP sample of 61.1% (the values of Raman crystallinity index are often lower than those measured by the X-ray diffraction method). CNF-CSR II had the highest CrI of 46%, perhaps due to incomplete acid hydrolysis and significantly fewer homogenization passes, 15 passes as compared to 47 passes used to produce CNF-M47p. The 4 h of additional milling in the SuperMassColloider destroyed more of the crystalline structure of cellulose, comparing CNF-S11h (CrI = 40.4%) with CNF-S7h (CrI = 43.4%). Typical values of Raman CrI of CNC are approximately 65% (Agarwal, U.P., private communication, USDA Forest Service, Forest Products Laboratory, 2012)

Optical and Mechanical Properties of CNF Films. At least five neat films were prepared from each CNF sample. Visual appearance of a particular neat film made of CNF-CSR II demonstrated excellent optical transparency in all colors (Figure 6), agreeing with spectral transmittance of the CNF suspension (Figure 4). As can be seen in Figure 7a, the optical opacities of the CNF films are decreased dramatically after nanofibrillation. The variability of CNF opacities are small among different CNF films though the opacity of the CNF film made from CSRs are lower (10–15%) than those CNF films made from the original BEP (~20%). While the opacity data agree with the spectral transmittance data of the CNF suspensions (Figure 4), the spectral transparency measurements showed significant variations among different CNF suspensions. No significant difference in CNF film opacity was observed with extended milling in the SuperMassCollodier from 7 h to 11 h.

Figure 6. Image of a film made of CNF-CSR II that shows its optical transparency in color. Thickness of the film is 60 μm.

Mechanical properties of neat films can only provide nominal information of CNF behavior; fiber network behavior depends on fiber geometry, especially length, fiber mechanical properties, and interfiber bonding. Specific tensile strengths and specific tensile moduli of the CNF neat films for the materials studied in this work were compared (Figure 7a,b). CNF-CSR I, CNF-CSR II, and CNF-M47p had statistically greater stiffness, based on analysis of variation (ANOVA) than CNF-S7h, CNF-S11h, and BEP 300 CSF. Relative ranking of stiffness agreed with DP results, i.e., the lowest DP had the greatest stiffness (CNF-CSR I) and the highest DP had the lowest stiffness (BEP 300 CSF). Amorphous regions were mostly eliminated in the strong acid hydrolysis for CNF-CSR I and CNF-CSR II, resulting in stiff and straight fibrils (Figure 5a,b). When compared with the tensile strength of the two CNFs from CSR produced under identical homogenization conditions (total of 15 passes), CNF-CSR II is stronger than the CNF-CSR I, probably due to greater fibril length, suggesting acid hydrolysis conditions may have affected fibril length. However, it is possible that less extensive mechanical homogenization may improve the strength of CNF-CSR. This will be studied in the future. CNF-CSR I and CNF-CSR II had statistically lower specific strengths, based on ANOVA, than CNF-M47p. CSR II had statistically greater strength than BEP 300 CSF while CNF-CSR I was statistically similar to BEP 300 CSF. Greater strength can be attributed to improved bonding, as demonstrated by the opacity of the film; improved bonding also increased stiffness, but straighter, less flexible fibrils of CNF-SCR II also made a critical contribution. The mechanical properties of CNF-CSR I and CNF-CSR II are quite encouraging, suggesting the residue product from CNC production waste stream is much stiffer without suffering strength loss. Properties of the film made from homogenized fibers, CNF-M47p, represent a good baseline for other CNFs but required significant mechanical energy for their production. Mechanical behavior of the films made from ground CNF, CNF-S7h and CNF-11h, scaled as expected. CNF-S11h had lower strength and stiffness caused by greater damage, mostly fiber shortening, in the grinder.

CONCLUSIONS

We recovered a new cellulosic material, CSR, from the waste stream of CNC production using acid hydrolysis. CSR was used

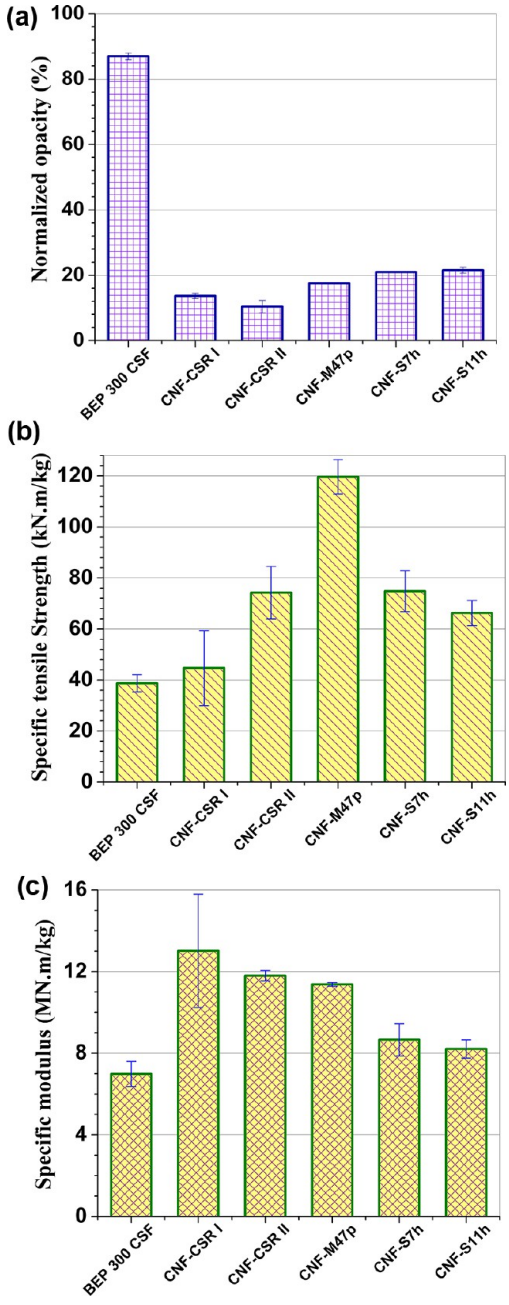

Figure 7. Optical and mechanical properties of CNF films: (a) opacity of cellulose nanofibrils films, (b) tensile strength, and (c) Young's modulus.

to produce cellulose nanofibrils (CNF) through mechanical fibrillation with significantly reduced energy input as compared with using bleached pulp. This CNF-CSR has a good spectral transparency, i.e, transmittance greater than 90% at wavelengths greater than 340 nm. When sulfuric acid is used, CSR contains sulfate groups that facilitate aqueous processing. Films formed from CNF-CSR show great good mechanical properties, with a specific tensile strength and modulus of 75 kN·m/kg and 12 MN·m/kg, respectively. Therefore, nanofilms made of CNF-CSR have potential applications such as flexible electronics and display.

Recovery of CSR from CNC production waste stream and the high value utilization of CSR, such as for CNF production as evaluated in this study, can significantly improve the

dx.doi.org/10.1021/am302967m | ACS Appl. Mater. Interfaces 2013, 5, 2527−2534

economics of CNC production. Effect of acid hydrolysis conditions and mechanical fibrillation on the optical and mechanical properties of CNF-CSR needs to be studied in the future. This study also demonstrated the feasibility to use acid hydrolysis as a standalone pretreatment step for CNF production to significantly reduce energy consumption for mechanical fibrillation.

AUTHOR INFORMATION

Corresponding Author

*Phone: (608) 231-9520. E-mail: jzhu@fs.fed.us.

Notes

The authors declare no competing financial interest.

This work was conducted on official government time of Zhu and Considine while Wang was a visiting student at the USDA Forest Service, Forest Products Laboratory.

ACKNOWLEDGMENTS

Financial support for this work included USDA Agriculture and Food Research Initiative (AFRI) Competitive Grant No. 2011-67009-20056 and the Chinese Scholarship Council (CSC). The funding from these two programs made the visiting appointment of Wang at the USDA Forest Products Laboratory (FPL) possible. We would like to acknowledge Fred Matt and Kolby Hirth (Both FPL) for conducting carbohydrate and sulfur content measurements, respectively, Thomas Kuster (FPL) for SEM image analysis, Debby Sherman of DS Imaging and the Life Science Microscopy Facility at Purdue University, and SAIC-Frederick, Inc., National Cancer Institute for TEM analysis.

REFERENCES

(1) Habibi, Y.; Lucia, L. A.; Rojas, O. J. *Chem. Rev.* **2010**, *110*, 3479−3500.
(2) Klemm, D.; Kramer, F.; Moritz, S.; Lindstrom, T.; Ankerfors, M.; Gray, D.; Dorris, A. *Angew. Chem., Int. Ed.* **2011**, *50*, 5438−5466.
(3) Eichhorn, S. J.; Dufresne, A.; Aranguren, M.; Marcovich, N. E.; Capadona, J. R.; Rowan, S. J.; Weder, C.; Thielemans, W.; Roman, M.; Renneckar, S.; Gindl, W.; Veigel, S.; Keckes, J.; Yano, H.; Abe, K.; Nogi, M.; Nakagaito, A. N.; Mangalam, A.; Simonsen, J.; Benight, A. S.; Bismarck, A.; Berglund, L. A.; Peijs, T. *J. Mater. Sci.* **2010**, *45*, 1−33.
(4) Šturcová, A.; Davies, G. R.; Eichhorn, S. J. *Biomacromolecules* **2005**, *6*, 1055−1061.
(5) Mark, R. E. In *Cell Wall Mechanics of Tracheids*; Yale University Press: New Haven, CT, 1967; p 119.
(6) Revol, J.-F.; Godbout, L.; Dong, X.-M.; Gray, D. G.; Chanzy, H.; Maret, G. *Liq. Cryst.* **1994**, *16*, 127−134.
(7) Roman, M.; Gray, D. G. *Langmuir* **2005**, *21*, 5555−5561.
(8) Dong, X. M.; Gray, D. G. *Langmuir* **1997**, *13*, 3029−3034.
(9) Rånby, B. G. *Discuss. Faraday Soc.* **1951**, *11*, 158−164.
(10) Mukherjee, S. M.; Woods, H.J. *Biochim. Biophys. Acta* **1953**, *10*, 499−511.
(11) Revol, J.-F.; Bradford, H.; Giasson, J.; Marchessault, R. H.; Gray, D. G. *Int. J. Biol. Macromol.* **1992**, *14*, 170−172.
(12) Bondeson, D.; Mathew, A.; Oksman, K. *Cellulose* **2006**, *13*, 171−180.
(13) Hamad, W. Y.; Hu, T. Q. *Can. J. Chem. Eng.* **2010**, *88*, 392−402.
(14) Wang, Q. Q.; Zhu, J. Y.; Reiner, R. S.; Verrill, S. P.; Baxa, U.; McNeil, S. E. *Cellulose* **2012**, *19*, 2033−2047.
(15) Spence, K. L.; Venditti, R. A.; Rojas, O. J.; Habibi, Y.; Pawlak, J. J. *Cellulose* **2011**, *18*, 1097−1111.
(16) Nakagaito, A. N.; Yano, H. *Appl. Phys. A* **2004**, *78*, 547−552.
(17) Syverud, K.; Stenius, P. *Cellulose* **2009**, *16*, 75−85.
(18) Siró, I.; Plackett, D.; Hedenqvist, M.; Ankerfors, M.; Lindström, T. *J. Appl. Polym. Sci.* **2011**, *119*, 2652−2660.
(19) Zhu, J. Y.; Sabo, R.; Luo, X. *Green Chem.* **2011**, *13*, 1339−1344.
(20) Henriksson, M.; Berglund, L. A.; Isaksson, P.; Lindström, T.; Nishino, T. D. *Biomacromolecules* **2008**, *9*, 1579−1585.
(21) Wang, Q. Q.; Zhu, J. Y.; Gleisner, R.; Kuster, T. A.; Baxa, U.; McNeil, S. E. *Cellulose* **2012**, *19*, 1631−1643.
(22) Stelte, W.; Sanadi, A. R. *Ind. Eng. Chem. Res.* **2009**, *48*, 11211−11219.
(23) Saito, T.; Kimura, S.; Nishiyama, Y.; Isogai, A. *Biomacromolecules* **2007**, *8*, 2485−2491.
(24) Henriksson, M.; Henriksson, G.; Berglund, L. A.; Lindström, T. *Eur. Polym. J.* **2007**, *43*, 3434−3441.
(25) Franson, M. H. In *Standard Methods for the Examination of Water and Wastewater*, 16th ed.; American Public Health Association (APHA): Washington, DC, 1985; p 532.
(26) *TAPPI Test Methods*; Technical Association of the Pulp and Paper Industry: Atlanta, GA, 2009.
(27) Alexander, W.; Goldschmid, O.; Mitchell, R. *Ind. Eng. Chem.* **1957**, *49*, 1303−1306.
(28) Mazumder, B.; Ohtani, Y.; Cheng, Z.; Sameshima, K. *J. Wood Sci.* **2000**, *46*, 364−370.
(29) Agarwal, U. P.; Reiner, R. S.; Ralph, S. A. *Cellulose* **2010**, *17*, 721−733.
(30) Mason, S. G. *Pulp Paper Mag. Can.* **1954**, *54*, 96−102.
(31) Kerekes, R. J.; Schell, C. J. *J. Pulp Paper Sci.* **1992**, *18*, 32−38.
(32) Celzard, A.; Fierro, V.; Kerekes, R. *Cellulose* **2009**, *16*, 983−987.